CHEMPHYSCHEM

DOI: 10.1002/cphc.200800007

# Silver Nanoparticle Thin Films with Nanocavities for Surface-Enhanced Raman Scattering

Mehmet Kahraman, Nilgün Tokman, and Mustafa Çulha*[a]

*The formation of nanometer-sized gaps between silver nanoparticles is critically important for optimal enhancement in surface-enhanced Raman scattering (SERS). A simple approach is developed to generate nanometer-sized cavities in a silver nanoparticle thin film for use as a SERS substrate with extremely high enhancement. In this method, a submicroliter volume of concentrated silver colloidal suspension stabilized with cetyltrimethylammonium bromide (CTAB) is spotted on hydrophobic glass surfaces prepared by the exposure of the glass to dichloromethysilane vapors. The use of a hydrophobic surface helps the formation of a more uniform silver nanoparticle thin film, and CTAB acts as a molecular spacer to keep the silver nanoparticles at a distance. A series of CTAB concentrations is investigated to optimize the interparticle distance and aggregation status. The silver nanoparticle thin films prepared on regular and hydrophobic surfaces are compared. Rhodamine 6G is used as a probe to characterize the thin films as SERS substrates. SERS enhancement without the contribution of the resonance of the thin film prepared on the hydrophobic surface is calculated as $2\times10^7$ for rhodamine 6G, which is about one order of magnitude greater than that of the silver nanoparticle aggregates prepared with CTAB on regular glass surfaces and two orders of magnitude greater than that of the silver nanoparticle aggregates prepared without CTAB on regular glass surfaces. A hydrophobic surface and the presence of CTAB have an increased effect on the charge-transfer component of the SERS enhancement mechanism. The limit of detection for rhodamine 6G is estimated as $1.0\times10^{-8}$ M. Scanning electron microscopy and atomic force microscopy are used for the characterization of the prepared substrate.*

## Introduction

Surface-enhanced Raman scattering (SERS) is a very powerful technique to obtain molecular information from chemical and biological molecules.[1–3] The "fingerprinting" property, limited influence of water, and high sensitivity make the technique very attractive for the characterization and detection of a variety of chemical and biological molecules and molecular structures. Since its discovery by Jeanmaire and Van duyne, Albrecht and Creighton, and Fleischmann et al.,[4–6] considerable effort has been devoted to the preparation of highly sensitive and reproducible SERS substrates. A number of strategies and methods for substrate preparation were reported based on the use of silver or gold colloidal suspensions,[7,8] surfaces prepared by deposition,[9] electrode surfaces,[4–6] and 2D[10] and 3D[11] array structures generated with lithographic methods.

Due to their major contribution to the SERS enhancement mechanism, surface plasmons are the focal point for the design of novel SERS substrates.[12] For the preparation of high-performing SERS substrates, parameters such as the size,[13–15] shape,[14–16] and type of noble metal,[15] aggregation properties,[14,17–21] and surface charge properties (zeta potential)[22] should be considered carefully. Recent studies have clearly indicated that the interparticle distance[14,19,23] is another critical parameter, and for optimum SERS enhancement the surface plasmons of the noble metal nanoparticles should overlap, which are called "hotspots". As a result of their stochastic nature, it is difficult to locate the hotspot sites in the aggregated silver nanoparticles when a colloidal suspension is used. Therefore, intense research has been undertaken on the construction of SERS substrates with predetermined hotspots[24,25] by using lithographic methods.

For hotspot formation, it is important for the nanoparticles to remain at a certain distance, which is typically in the range of 1–4 nm.[26–28] However, as several factors, such as the size, shape, surface morphology, and type of the noble metal and wavelength of the laser light, may influence the formation and range of surface plasmons, the interparticle distance may vary depending on the system under investigation. Emory et al. found that when the particle size was increased, a longer-wavelength laser light was needed to obtain higher enhancement.[13] Kneipp et al. investigated the aggregation properties of silver and gold nanoparticles and their SERS performance.[21,29] They demonstrated that a near-infrared (NIR) laser wavelength was necessary for optimal enhancement, as the nanoparticles were aggregated.[21] It is now clear that surface plasmons of nanoparticles shift to longer wavelengths due to aggregation of the nanoparticles,[29] and Raman enhancement is independent of the aggregate size after about 1 μm in cases where aggregates are formed.[30]

The surface-charge properties of the nanoparticles are also critical for the adsorption of molecules on the nanoparticle sur-

[a] M. Kahraman, Dr. N. Tokman, Prof. Dr. M. Çulha
Department of Genetics and Bioengineering
Faculty of Engineering and Architecture
Yeditepe University, 34755 Kayisdagi-Istanbul (Turkey)
Fax: (+90) 216-578-00-40
E-mail: mculha@yeditepe.edu.tr

  

face[22,31] and the degree of aggregation.[32] For instance, gold or silver colloidal suspensions prepared by a citrate reduction method possess a negative charge due to the adsorption of the citrate anions on the nanoparticles. The aggregation of such particles can be induced by addition of positively or negatively charged ions or molecules due to their influence on the electrical double layer.[32] To control the aggregation properties, the use of halide ions, such as $Cl^-$ and $Br^-$,[33,34] and other additives[18,35,36] was studied. Analyte adsorption on the nanoparticle surfaces was also examined by changing the charge of the analyte to increase interaction between the molecule of interest and the nanoparticles.[37]

The difficulty in controlling the aggregation of colloidal gold or silver nanoparticles results in the irreproducibility of the SERS substrate, and thus the acquired SERS spectra. To avoid the problems associated with the use of colloidal nanoparticles as SERS substrates, other approaches, for example mirror reaction,[38] vapor deposition,[39,40] and 3D structures or arrays using different methods such as lithographic and convective assembly,[41–45] were explored. However, these methods also have drawbacks, such as low enhancement factor, difficulty in the reproducible preparation of the patterned surfaces, and sometimes high cost due to the use of sophisticated lithographic methods.

The development of stable, reproducible, cost-effective, highly enhancing, and easily prepared SERS substrates is still under intense investigation. While all of these properties are important, a high enhancement factor is especially critical for the detection and analysis of low-concentration analytes. Although the feasibility of single-molecule detection on the aggregates of silver and gold nanoparticles with a $1.0\times10^{14}$ enhancement factor was reported,[46,47] almost all commercially available SERS substrates have an enhancement factor in the range of $1.0\times10^4$–$1.0\times10^5$. Recently, a number of SERS substrates were prepared by several different methods with enhancement factors ranging from $1.0\times10^4$ to $1.0\times10^7$. There has only been one report claiming an enhancement factor of $10\times10^{11}$ since the earlier two reports.[48–55]

Herein, we demonstrate the preparation of a reproducible, low-cost, highly enhancing SERS substrate by controlling the aggregation and interparticle distance using cetyltrimethylammonium bromide (CTAB) molecules as spacers on a hydrophobic surface with concentrated silver nanoparticles. The enhancement factor, limit of detection (LOD), and reproducibility of the prepared substrate were investigated by using rhodamine 6G. Atomic force microscopy (AFM) and scanning electron microscopy (SEM) are used to characterize the prepared SERS substrates.

## Results and Discussion

Silver or gold colloidal suspensions have been widely used as SERS substrates due to their simple preparation procedures and low cost. In a typical SERS experiment, an analyte is placed on a spot generated from a droplet of colloidal suspension or mixed with the colloidal suspension and then spotted on a substrate. In either case, the aggregation properties of the colloidal nanoparticles are critical for optimum SERS enhancement and there is almost always no control of aggregation, especially when the colloidal suspension is mixed with the analyte. In the case of spotting the analyte on a thin-film surface prepared from a colloidal suspension, the change of SERS activity with the concentration of the analyte could be a factor due to possible changes in aggregation properties, as observed in this study. Although this effect might be dependent on the chemical nature of the analyte, increased rhodamine 6G concentrations had a positive influence on the SERS enhancement due to the fact that an 830 nm laser wavelength was used and the formation of surface plasmons shifted towards the longer wavelength. This finding can be explained by the increased aggregation of silver nanoparticles as the droplet of rhodamine 6G solution placed on the silver nanoparticle thin film dries.

Although it does not eliminate the irreproducibility of the SERS spectra, an increased concentration of the colloidal suspension improves the SERS enhancement of the substrate due to the increased aggregation. Our previous study demonstrated that the use of a hydrophobic surface prepared by exposing the surface of a glass slide to dichloromethylsilane vapors helped the formation of silver nanoparticle aggregates with a definite size (see Figure 2D). The silver nanoparticles used in that study were citrate-reduced and their surface charge was predominantly negative. Locating a concentrated silver colloidal suspension on hydrophobic surfaces forces the negatively charged and water solvated silver nanoparticles to form aggregates with a size of about 1.0 μm. In the present study, we aim to prepare a uniform silver nanoparticle film with molecule-sized pores. The expectation from such a structure is a tremendous SERS enhancement due to the extensive overlapping of surface plasmons of silver nanoparticles in the aggregates.

The adsorption of CTAB onto silver nanoparticles was studied.[57] The CTAB molecule has a positively charged head group and hydrophobic tail. The surface charge of the silver nanoparticles used in this study is negative due to the presence of the citrate ions. The addition of CTAB molecules to the citrate-reduced colloidal suspension results in the adsorption of the CTAB molecules onto the silver nanoparticles through the positively charged head groups. With this type of orientation, CTAB can act as a molecular spacer between the aggregating silver nanoparticles. To investigate whether the adsorption of CTAB occurs on top of citrate ions or after the citrate ions are desorbed, the SERS spectra before and after the addition of CTAB to the colloidal suspension are acquired (see Figure 1). The SERS spectrum of citrate ions on silver nanoparticles is typical, and agrees quite well with the reported spectra.[58,59] After the addition of CTAB molecules to the suspension, the SERS spectrum obtained from the silver colloidal suspension completely changes, which suggests that at least some of the citrate ions are desorbed from the silver nanoparticle surface.

The formation of a monolayer and multilayers on a silver electrode surface has been studied using SERS.[60] Inspection of the SERS spectra in Figure 1 reveals that the CTAB molecules are adsorbed onto the silver nanoparticle surfaces through their positively charged head groups. Importantly, a broad con-

  

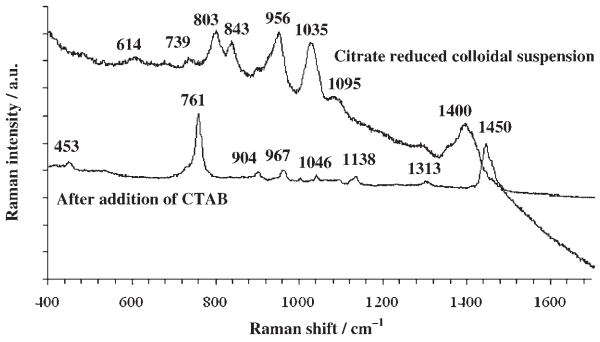


**Figure 1.** SERS spectra of citrate ions on colloidal silver nanoparticles and after the addition of CTAB to the colloidal suspension (CTAB concentration: 1 mM in the solution).

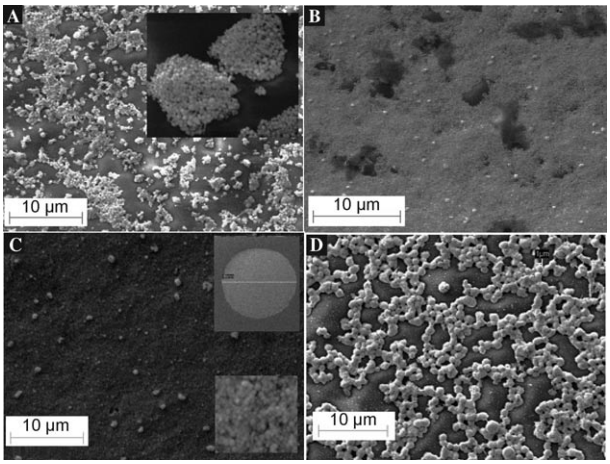


**Figure 2.** SEM images of substrates prepared on a hydrophilic glass surface without (A) and with CTAB (B) and on a hydrophobic surface with 1 mM CTAB (C) and without CTAB (D). For all images, the colloidal suspension concentration is 32×. The inset images show the structures at high magnification (A and C) and the whole spot area (C).

tinuum background is observed, especially with the citrate spectrum. This is due to the magnitude of the extinction of the laser irradiation by the concentrated silver nanoparticles and possible coupling to surface plasmon resonances. This phenomenon was observed in the history of early SERS experiments,[61,62] and this optical continuum has recently been correlated with a single-molecule SERS effect.[63,64] Notably, the presence of CTAB diminishes this effect, possibly due to its influence on the degree of aggregation and on the surface plasmons as a result of the changes in surface-charge properties of the silver nanoparticles. However, the presence of CTAB molecules does not completely eliminate the observed background effect. The two intense and broad peaks at 1450 and 760 cm$^{-1}$ can be assigned to N–$CH_3$ symmetric and asymmetric bending, and $CH_3$ rocking from the $N^+(CH_3)_3$ group. The other weaker peaks at 904, 967, 1046, and 1138 cm$^{-1}$ can be attributed to C–$N^+$ stretching, C–$N^+$ stretching, C–C symmetric stretching, and C–C asymmetric stretching, respectively.[60,65] These peak assignments suggest that the CTAB molecules are indeed adsorbed through their positively charged head groups onto the silver nanoparticles, as suggested by a previous study.[57]

As mentioned above, an increased concentration of colloidal suspension has a considerable impact on the SERS enhancement of colloidal silver nanoparticles spotted and dried on surfaces. Several concentrations of the colloidal suspension were investigated for optimum SERS performance and complete surface coverage of the spot area. It is found that the 32× concentrated colloidal suspension is superior for SERS enhancement, and almost completely covered the spot area and formed a very uniform thin film. Figure 2 shows SEM images of the spots of the 32× concentrated colloidal suspension on untreated and hydrophobic glass surfaces without and with CTAB. While the arbitrary aggregation of silver colloidal nanoparticles on the untreated glass surface is clearly seen, the colloidal silver nanoparticles form a very uniform thin film on the hydrophobic surface. An inset of Figure 2C shows an image of the spot on the hydrophobic surface; it is almost perfectly round in shape with an average diameter of 1.6 ± 0.1 mm. This easy spot-size control combined with controlled colloidal suspension concentration generates a very uniform film density. The formation of a uniform silver thin film can be explained in terms of the presence of a hydrophobic surface and partially hydrophobic silver nanoparticle surface due to the presence of CTAB molecules in the suspension. A hydrophobic surface confines the colloidal droplet on a limited area by preventing the spread of the droplet, while the silver nanoparticles are distributed on the hydrophobic surface and remain at a certain distance from each other, predicted by the layers of CTAB molecules as water evaporates from the droplet.

Due to its superior SERS performance compared to lower concentrations and complete surface coverage on the spot area, the 32× concentrated silver colloidal suspension was used for further experiments. The concentration of CTAB was optimized for maximum SERS enhancement by varying the CTAB concentration. As mentioned earlier, the addition of rhodamine 6G solution to the surface prepared from colloidal suspension may further influence the aggregation of silver nanoparticles in the thin film. An increase in aggregation may result in increased SERS activity due to a shift of surface plasmon formation frequency closer to the laser wavelength frequency (830 nm in this study). Therefore, a dilute rhodamine 6G solution ($1.0\times10^{-6}$ M) was used for the experiments to limit the influence of aggregation caused by the added analyte and to observe the influence of the presence of CTAB.

Figure 3 shows the SERS spectra of rhodamine 6G at three different CTAB concentrations. Overall, the intensity of the peaks of rhodamine 6G obtained from the spot of colloidal suspension prepared with $1.0\times10^{-3}$ M CTAB was about tenfold higher than for $1.0\times10^{-4}$ M CTAB and about twofold higher than for $1.0\times10^{-2}$ M CTAB, which indicates that the optimum CTAB concentration falls around $1.0\times10^{-3}$ M. Interestingly, this concentration is around the critical micelle concentration (CMC) of CTAB. When CTAB is added to obtain $1.0\times10^{-4}$ M as a final concentration in the suspension, the silver colloidal suspension collapses and almost loses its SERS activity. This could be due to the neutralization of negatively charged citrate ions by positively charged CTAB molecules and the formation of a

  

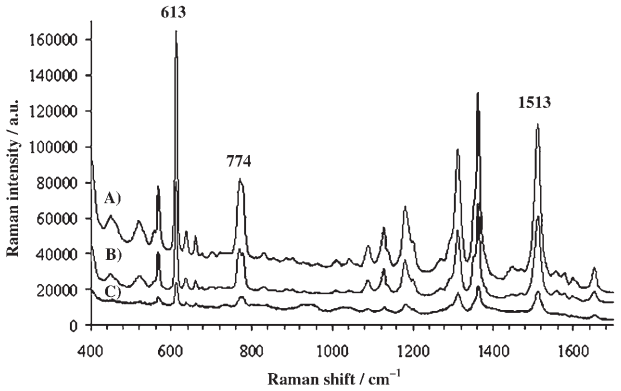


**Figure 3.** SERS spectra of a hydrophobic surface with different concentrations of CTAB A) $1.0\times10^{-3}$ M B) $1.0\times10^{-2}$ M C) $1.0\times10^{-4}$ M in 32× silver colloidal suspension. Laser power: 1.5 mW, rhodamine 6G: 0.5 μL $1.0\times10^{-6}$ M, exposure time: 10 s, accumulation: 1.

complete monolayer of CTAB molecules on the silver nanoparticles, thus generating a mostly hydrophobic surface. The lack of dominant negative or positive charges on the silver nanoparticles stabilizing the colloidal suspension may induce the collapse of the suspension.

The number of CTAB molecules on single silver nanoparticles can be estimated from the final concentrations of the silver nanoparticles and CTAB in 0.5 μL of suspension, which was spotted on the hydrophobic surface. Assuming that the density of the silver colloidal suspension is $2\times10^{11}$ particles per mL, the number of silver nanoparticles in 0.5 μL of 32× concentrated suspension is estimated to be $3.2\times10^{8}$. At a CTAB concentration of 1 mM, the number of CTAB molecules per nanoparticle is estimated as $9.4\times10^{4}$. The length of the CTAB molecule was reported to be about 2 nm.[66] The size of the positively charged head group adsorbed on silver nanoparticle surfaces is estimated as 0.36 nm from the size of the whole CTAB molecule. The number of CTAB molecules that form a monolayer on the surface of a silver nanoparticle of size 50 nm is $2.61\times10^{5}$. The total number of CTAB molecules forming a monolayer in 0.5 μL of 32× concentrated colloidal suspension can be estimated as $8.3\times10^{13}$ ($3.2\times10^{8}$ particles $\times 2.61\times10^{5}$ molecules per particle). The total number of CTAB molecules in 0.5 μL of colloidal suspension is $3.1\times10^{14}$.

These calculations indicate that there are more than enough CTAB molecules to form a monolayer in the suspension, and it may not be incorrect to assume that there is an incomplete second layer on the surface of the silver nanoparticles. In this layer, some of the CTAB molecules could be interacting through their hydrophobic tails with the hydrophobic tails of the CTAB molecules adsorbed on the silver nanoparticles. This generates a partially positively charged nanoparticle surface that stabilizes the colloidal suspension, and this partial bilayer acts as a molecular spacer between silver nanoparticles. Considering the size of CTAB molecules, the size of the molecular pores can be assumed to be in the range of 2–4 nm, which is an excellent gap size for surface plasmon overlap. The CTAB molecules interact with the hydrophobic surface through their hydrophobic tails and generate a positively charged surface. This helps the spread of partially positively charged silver nanoparticles on the hydrophobic surface. Figure 4 shows the proposed model for the silver nanoparticle thin film on the hydrophobic surface. Notably, the treatment of the hydrophobic surface with CTAB solution before spotting the colloidal suspension without added CTAB does not generate a uniform film (see Figure 6C).

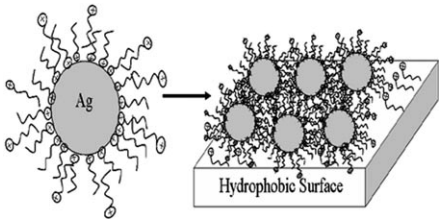


**Figure 4.** Structure of the silver thin film.

The charge and the molecular structure of the analyte could play an important role in the SERS experiment as well. For example, a rhodamine 6G molecule is mostly hydrophobic with a positive charge. When the surface charge of the nanoparticles is partially positive, it may diffuse into the molecule-sized porous structure of the colloidal silver nanoparticle film. The presence of a completely positive charge on the nanoparticle surface may hinder the deeper penetration of a positively charged rhodamine 6G molecule due to repulsion forces. The decrease in the SERS performance of silver nanoparticle films prepared with concentrations higher ($1.0\times10^{-2}$ M) than the CMC can be explained by the higher density of positive charges on the nanoparticle surface. This may prevent the diffusion of the rhodamine 6G molecule into the thin-film structure and it may remain mostly on the surface. Therefore, it cannot completely benefit from surface plasmons of silver nanoparticles.

The presence of a layer of molecules on the surface of the silver nanoparticles may influence the charge-transfer component of the SERS enhancement mechanism. The peaks on the rhodamine 6G SERS spectrum at 614 and 773 cm$^{-1}$ are out-of-plane modes, which are due to vibronically coupled charge-transfer contributions to SERS.[67] The inspection of spectra of rhodamine 6G acquired from an aggregate prepared from 32× colloidal suspension on a glass surface and on a hydrophobic surface, and thin films prepared from colloidal suspensions with CTAB concentrations of $1.0\times10^{-3}$ M, $1.0\times10^{-2}$ M, and $1.0\times10^{-4}$ M, revealed that there could be some contributions to the SERS enhancement mechanism from the charge transfer. The ratios of the peak heights ($I_{614}/I_{1513}$ and $I_{773}/I_{1513}$) at 614 and 773 cm$^{-1}$ with respect to the peak at 1513 cm$^{-1}$, which is an in-plane mode, are given in Table 1. Interestingly, there is not a significant difference in the peak-height ratio values for the hydrophobic and hydrophilic glass surfaces in the absence of CTAB, while there is a considerable increase in the intensity ratio values on the aggregates prepared from the silver colloi-

  

**Table 1.** Peak-height ratios of rhodamine 6G peaks at 614 and 773 $cm^{-1}$ with respect to 1513 $cm^{-1}$.

| Surface | [CTAB] [M] | $I_{614}/I_{1513}$ | $I_{773}/I_{1513}$ |
|---|---|---|---|
| Plain glass | – | 1.10 | 0.42 |
| | $10^{-3}$ | 0.41 | 0.51 |
| Hydrophobic | – | 1.09 | 0.46 |
| | $10^{-4}$ | 1.24 | 0.26 |
| | $10^{-3}$ | 1.45 | 0.52 |
| | $10^{-2}$ | 1.35 | 0.52 |

dal suspension containing CTAB. Comparison of the $I_{614}/I_{1513}$ value obtained from thin films prepared from colloidal suspension containing $10^{-3}$ M CTAB indicates that the formation of the thin film on a hydrophobic surface could have a significant effect on the charge-transfer component of the SERS enhancement mechanism. The comparison of the peak ratios obtained from SERS spectra acquired from thin films prepared with colloidal suspension containing three different CTAB concentrations on the hydrophobic surface indicates that the charge-transfer contribution with $10^{-3}$ M CTAB to the SERS enhancement mechanism is the largest. Overall, it can be concluded that both a hydrophobic surface and a critical CTAB concentration influence the charge-transfer component of the SERS mechanism.

Figure 5 shows the SERS performance of silver thin films prepared on hydrophobic and hydrophilic surfaces. The trend with increasing concentration of the colloidal suspension is very dramatic, and the increase with the 32× concentration is the greatest on both surfaces due to a higher degree of aggregation of silver colloidal nanoparticles. A higher degree of aggregation results in a higher possibility of overlapping surface plasmons of nanoparticles at the particle junctions. A comparison of the peak intensities at 1512 $cm^{-1}$ indicates that a minimum fivefold increase in the SERS signal of rhodamine 6G was obtained on the hydrophobic surface at almost all concentrations. Notably, even with the increased concentration of colloidal suspension, the aggregates on the hydrophilic glass surfaces should be targeted through the surface plasmons of aggregates under the microscope objective for comparable spectral acquisition. However, on the hydrophobic surfaces this is almost unnecessary due to a very uniform film. The location of the laser beam on any point on the thin film is satisfactory for reproducible SERS spectra.

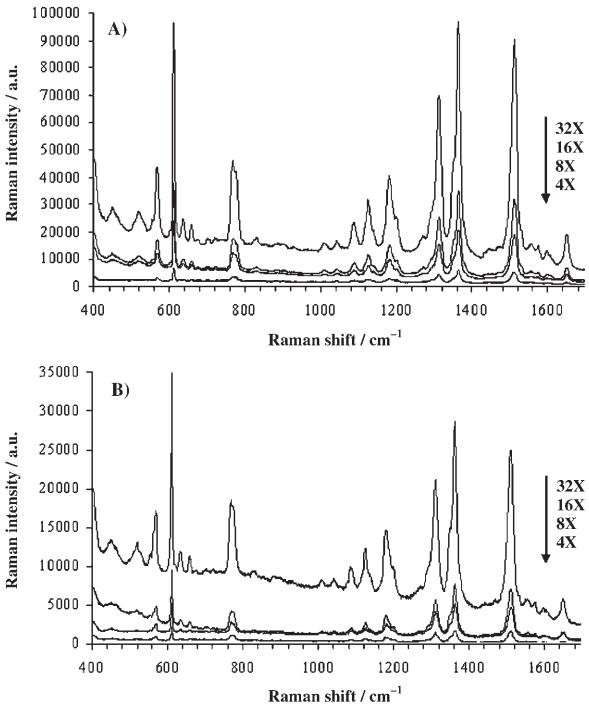


**Figure 5.** Performance of silver colloidal thin films prepared with increased colloidal concentrations on A) hydrophobic and B) hydrophilic surfaces. The final concentration of CTAB in all experiments is $1.0\times10^{-3}$ M.

As the thin film is prepared of silver nanoparticles, the surface roughness, investigated by AFM gives indirect information about its structure. Figure 6 shows AFM images and surface roughness of thin films prepared from 32× concentrated silver colloidal suspension with CTAB on a hydrophobic surface, a plain glass surface, and a hydrophobic surface but with the $1.0\times10^{-3}$ M CTAB spotted on it and then 32× colloidal suspension prepared without CTAB added. In Figures 6A–C, the surface roughness profiles along the red and green labeled lines are seen on the right-hand side. The AFM images indicate that the surface roughness in Figure 6A is much greater and the particle size distribution much narrower than for the surfaces seen in Figure 6B and C. Combined with the fact that the thin film is prepared from silver nanoparticles and the nanoparticle surfaces were covered with CTAB molecules, the surface roughness can be related to the structure of the thin film. Besides, the interparticle distance smaller than 1 nm significantly reduces the SERS activity of the structures.[26–28] The lower SERS activity of the silver nanoparticle aggregates prepared from colloidal suspension without CTAB indicates the smaller distances among the silver particles forming the aggregates. Therefore, we hypothesize that there are nanometer-sized gaps or cavities between the silver nanoparticles in the film structure, which form a porous structure.

When the silver colloidal suspension containing CTAB is spotted on the hydrophobic surface, the CTAB molecules could be adsorbed on the surface through their hydrophobic tails to form a monolayer. To investigate the influence of the formation of this monolayer on the SERS performance of the silver nanoparticle aggregates, the hydrophobic surface is treated with 1 mM CTAB solution and a silver colloidal suspension with the same concentration (32×) is spotted on the hydrophobic surface. Figure 7 shows the SERS spectra of rhodamine 6G obtained from both surfaces. It is apparent that the generation of a positively charged surface due to the formation of a monolayer of CTAB molecules does not influence the SERS performance of the silver thin film prepared from colloidal suspension without CTAB. This finding indicates that the presence of CTAB molecules in the colloidal suspension causes the formation of molecule-sized gaps between the silver nanoparticles. The lack of such nanocavities in the thin films not only prevents the diffusion of analyte molecules into the cavities but also the formation of overlapping surface plasmons.

  

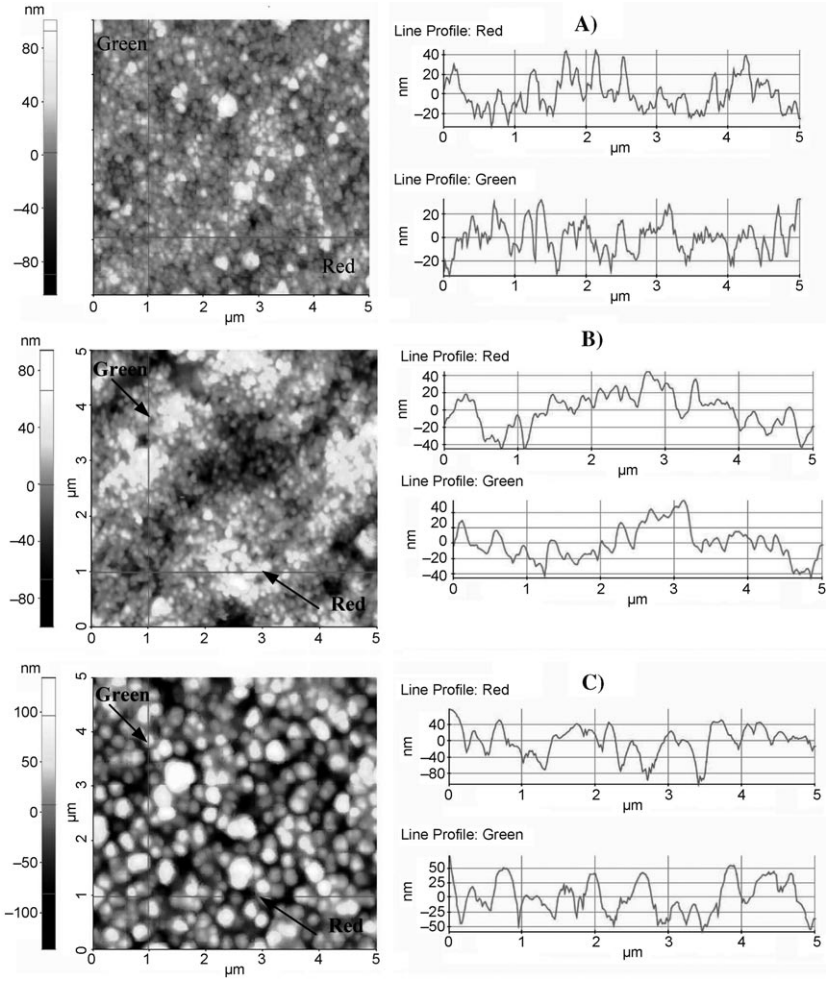


**Figure 6.** AFM images of the substrates prepared from 32× concentrated silver colloidal suspension containing 1 mM CTAB on A) hydrophobic surface and B) glass surface, and C) hydrophobic surface but with $1.0\times10^{-3}$ M CTAB spotted on it and then 32× colloidal suspension prepared without added CTAB.

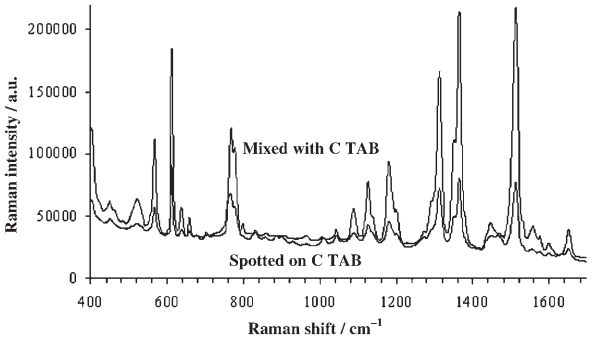


**Figure 7.** Comparison of the SERS performance of thin films prepared from 32× concentrated colloidal suspension containing CTAB and those prepared from a similar suspension without CTAB on the hydrophobic surface treated with $1.0\times10^{-3}$ M CTAB. Laser power: 3 mW, rhodamine 6G: 0.5 μL 1 μM, exposure time: 10 s, accumulation:1.

### Limit of Detection (LOD)

The LOD of the prepared SERS substrate for rhodamine 6G is estimated as $1.0\times10^{-8}$ M using a series of concentrations. For clarity, the higher and lower concentrations are presented in Figures 8A and B, respectively. Figure 8B also shows the background SERS spectrum. Most of the rhodamine 6G peaks are easily separated from the background peaks down to a concentration of $1.0\times10^{-8}$ M.

To approximate the number of rhodamine 6G molecules contributing to the SERS signal, the number of rhodamine 6G molecules per silver nanoparticle is estimated. Assuming the laser spot size is about 1 μm and the thin-film spot size is 1.6 ± 0.1 mm, the number of silver nanoparticles in a thin film prepared from a 32× concentrated colloidal suspension under the impinging laser light is 1280. The density of the silver colloidal suspension is $2.0\times10^{11}$ particles per mL as synthesized.[56] Since the minimum detectable concentration of rhodamine 6G is $1.0\times10^{-8}$ M, the number of rhodamine 6G molecules under the laser light is 1204 with the assumption that the rhodamine 6G molecules form a uniform monolayer in the silver thin film. When 0.5 μL of rhodamine 6G solution is spotted on the prepared silver nanoparticle thin film, the solution completely covers all the 2.0 mm$^2$ area of the thin film. Therefore, the density of rhodamine 6G is roughly estimated as one molecule per silver nanoparticle in the thin film. Due to the fact that only a small fraction of rhodamine 6G molecules contribute to the SERS signal, the detectable concentration is smaller than the observed concentration.

### Enhancement Factor and Reproducibility

The peak at 1512 cm$^{-1}$ is used to calculate the enhancement factor. Rhodamine 6G solutions at concentrations of $1.0\times10^{-1}$ and $1.0\times10^{-6}$ M are used for the bulk Raman and SERS experiments, respectively. The intensity ratio is calculated as 195 and the concentration factor as $1.0\times10^{5}$. The enhancement factor, estimated by application of the formula $I_{SERS}/I_{Bulk}\times C_{Bulk}/C_{SERS}$, is $2.0\times10^{7}$. This enhancement factor is also consistent with a 2–4 nm interparticle distance.[23] Figures 9A and B show the bulk

  

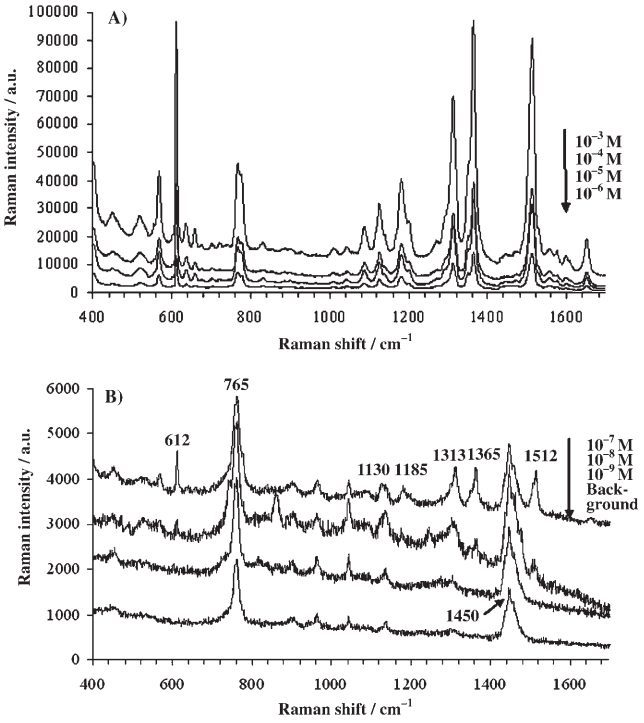


**Figure 8.** SERS spectra of rhodamine 6G with decreasing concentrations: A) higher concentrations and B) lower concentrations, which were separated for clarity. Laser power: 0.3 mW, rhodamine 6G: 0.5 μL, exposure time:10 s, accumulation: 1.

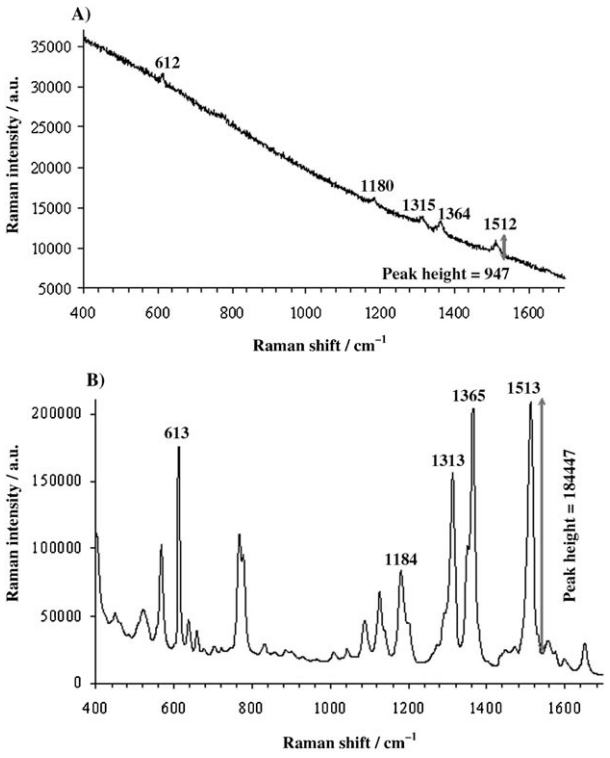


**Figure 9.** A) Bulk Raman and B) SERS spectra of rhodamine 6G. Laser power: 3 mW, 2 μL 100 mM rhodamine 6G for bulk Raman and 0.5 μL $1.0\times10^{-6}$ M rhodamine 6G for SERS experiments (the substrate was prepared under optimal conditions), exposure time: 10 s, accumulation: 1.

Raman and SERS spectra of rhodamine 6G, respectively. Notably, the laser wavelength used in this study is 830 nm. There are several reasons for using a NIR laser with silver colloidal nanoparticles. First of all, as silver nanoparticles form aggregates, the resonance for surface plasmons becomes almost independent of laser wavelength. The use of a laser wavelength in the UV/Vis region could be destructive for the molecule under investigation, whereas the use of a NIR wavelength could increase the sensitivity further due to its greater penetration depth. Finally, a NIR laser is more suitable for the investigation of biological molecules and structures.[68,69] Indeed, up to $10^{14}$ times enhancement is reported for silver nanoparticle aggregates with the use of a NIR laser (780 nm).[47] The estimated enhancement factor in this study is free of the contribution from resonance because rhodamine 6G does not have a chromophore absorbing at 830 nm.

The spot-to-spot reproducibility of the SERS spectra for the substrate, shown in Figure 10 for ten arbitrarily chosen different spots on the thin film, is excellent. The coefficients of variation of peak height, absolute intensity, and area at 1512 cm$^{-1}$ are 1.63, 1.68, and 2.37, respectively. The substrate is SERS-active for several days.

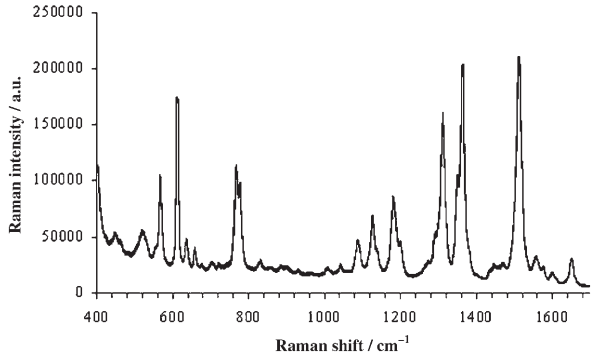


**Figure 10.** SERS spectra of rhodamine 6G taken at ten different spots on the same substrate. Laser power: 3 mW, rhodamine 6G: 0.5 μL $1.0\times10^{-6}$ M, exposure time: 10 s, accumulation: 1.

## Conclusions

We have reported a simple, reproducible, and ultrasensitive SERS substrate preparation method. With this approach, the interparticle distance of silver nanoparticles in the aggregates can be controlled. The technique is based on the preparation of a silver nanoparticle thin film on hydrophobic surfaces using a concentrated silver colloidal suspension containing CTAB. The optimum concentration of the suspension was obtained by concentrating the synthesized silver colloidal suspension 32 times. The final concentration of CTAB in the colloidal suspension was 1 mM for maximum SERS enhancement. The SERS enhancement obtained from the silver thin films prepared from the CTAB-containing colloidal suspension on the hydrophobic surface was one order of magnitude greater than for a hydrophilic glass surface. It is also found that the thin film prepared

  

on a hydrophobic surface from a colloidal suspension containing CTAB at a concentration around the CMC may help to increase the charge-transfer contribution to the SERS enhancement mechanism. The LOD and enhancement factor were estimated as $1.0\times10^{-8}$ M and $2\times10^{7}$, respectively, on the hydrophobic surface with the 32× concentrated silver nanoparticle suspension containing $1.0\times10^{-3}$ M CTAB. This method is simple and cost effective. A very sensitive and reproducible SERS-active surface can be prepared in a very short time.

## Experimental Section

Materials: Silver nitrate was purchased from Fluka (Seelze, Germany). CTAB and trisodium citrate were obtained from Merck (Darmstadt, Germany). Dichloromethylsilane and rhodamine 6G were purchased from Alfa Aesar (Karlsruhe, Germany). All chemicals were used as received.

Preparation of Silver Nanoparticles: The silver colloidal suspension was prepared using the method of Lee and Meisel.[7] Briefly, $AgNO_3$ (90 mg) was dissolved in water (500 mL) and heated to boiling point. An aliquot (10 mL) of 1% sodium citrate was added to the solution, which was kept boiling until the volume reached half of the initial volume. The maximum absorption of the solution was recorded at 420 nm. In this method, the density of the silver particles is $2.0\times10^{11}$ particles per mL and the average particle size is 40–60 nm.[56] The silver colloidal suspension was concentrated 4, 8, 16, and 32 times by centrifugation at 5500 rpm for 30 min.

Preparation of SERS Substrate: Regular glass slides were left overnight in a chromic acid solution and washed by submerging in distilled water. The cleaned glass slides were used to prepare the hydrophobic surfaces by exposing them to dichloromethylsilane ($CH_3SiHCl_2$) in a closed container. The concentrated silver colloids with or without CTAB were spotted on the regular glass surface (hydrophilic) and hydrophobic glass surface.
Silver colloidal solutions containing CTAB were prepared by the addition of a suitable amount of CTAB to the colloidal suspensions. To investigate the concentration effect of CTAB on SERS performance, three different concentrations (one above, one below, and one around the CMC) were prepared at $1.0\times10^{-2}$, $1.0\times10^{-3}$, and $1.0\times10^{-4}$ M, respectively. Moreover, the same CTAB concentrations were investigated by spotting on the hydrophobic surface first and then the silver colloidal suspension without CTAB was added on the same surface. A range of rhodamine 6G concentrations of $1.0\times10^{-3}$–$1.0\times10^{-9}$ M was used in the LOD experiments. The SERS enhancement factor was estimated by comparing $1.0\times10^{-1}$ M rhodamine 6G (2 μL) for the bulk Raman experiment and $1.0\times10^{-6}$ M rhodamine 6G (0.5 μL) for the SERS experiment. All SERS experiments were performed by the addition of rhodamine 6G solution to the silver colloidal thin film unless stated otherwise.

Raman Instrumentation: A Renishaw inVia reflex Raman microscopy system was used to perform all SERS experiments. The system was automatically calibrated against a silicon wafer peak at 520 $cm^{-1}$. A diode laser at 830 nm and a 50× objective (numerical aperture: 0.75) with a laser power of 0.3 mW were used for all experiments, with the exception that the laser power was 3 mW for the enhancement factor experiments and substrates prepared with CTAB.
Microscopy: All SEM images were obtained using a Carl Zeiss Evo 40 instrument at high vacuum and extra-high tension (10 kV). AFM images were obtained with a Park Systems XE-100 instrument using the noncontact mode.

## Acknowledgements

*The financial support from Yeditepe University Research Fund and TUBITAK is greatly acknowledged.*

**Keywords:** aggregation · colloids · nanoparticles · silver · surface-enhanced Raman scattering

[1] S. Lee, S. Kim, J. Choo, S. Y. Shin, Y. H. Lee, H. Y. Choi, S. Ha, K. Kang, C. H. Oh, *Anal. Chem.* **2007**, *79*, 916–922.
[2] C. Ruan, W. Wang, B. Gu, *Anal. Chem.* **2006**, *78*, 3379–3384.
[3] O. Cozar, N. Leopold, C. Jelic, V. Chis, L. David, A. Mocanu, M. Tomoaia-Cotisel, *J. Mol. Struct.* **2006**, *788*, 1–6.
[4] D. J. Jeanmaire, R. P. Van Duyne, *J. Electroanal. Chem.* **1977**, *84*, 1–20.
[5] M. Fleischmann, P. J. Hendra, A. J. McQuillan, *Chem. Phys. Lett.* **1974**, *26*, 163–166.
[6] M. G. Albrecht, J. A. Creighton, *J. Am. Chem. Soc.* **1977**, *99*, 5215–5217.
[7] P. C. Lee, D. Meisel, *J. Phys. Chem.* **1982**, *86*, 3391–3395.
[8] J. A. Creighton, C. G. Blatchford, M. G. Albercht, *J. Chem. Soc. Faraday Trans. 2* **1979**, *75*, 790–798.
[9] S. Kubo, Z.-Z. Gu, D. A. Tryk, Y. Ohko, O. Sato, A. Fujishima, *Langmuir* **2002**, *18*, 5043–5046.
[10] M. K. Hossaina, K. Shibamotoc, K. Ishioka, M. Kitajimaa, T. Mitanid, S. Nakashima, *J. Lumin.* **2007**, *122–123*, 792–795.
[11] L. Lu, I. Randjelovic, R. Capek, N. Gaponik, J. Yang, H. Zhang, A. Eychmüller, *Chem. Mater.* **2005**, *17*, 5731–5736.
[12] M. Moskovits, *Rev. Mod. Phys.* **1985**, *57*, 783–826.
[13] S. R. Emory, W. E. Haskins, S. Nie, *J. Am. Chem. Soc.* **1998**, *120*, 8009–8010.
[14] T. Jensen, L. Kelly, A. Lazarides, G. C. Schatz, *J. Cluster Sci.* **1999**, *10*, 295–317.
[15] E. J. Zeman, G. C. Schatz, *J. Phys. Chem.* **1987**, *91*, 634–643.
[16] J. Zhang, X. Li, X. Sun, Y. Li, *J. Phys. Chem. B* **2005**, *109*, 12544–12548.
[17] A. N. Shipway, M. Lahav, R. Gabai, I. Willner, *Langmuir* **2000**, *16*, 8789–8795.
[18] G. Wei, H. Zhou, Z. Liu, Z. Li, *Appl. Surf. Sci.* **2005**, *240,* 260–267.
[19] K. Kneipp, H. Kneipp, I. Itzkan, R. R. Dasari, M. S. Feld, *J. Phys. Condens. Matter* **2002**, *14*, 597–624.
[20] K. Kneipp, H. Kneipp, I. Itzkan, R. R. Dasari, M. S. Feld, *Chem. Rev.* **1999**, *99*, 2957–2975.
[21] K. Kneipp, H. Kneipp, R. Manoharan, E. Hanlon, I. Itzkan, R. R. Dasari, M. S. Feld, *Appl. Spectrosc.* **1998**, *52,* 1493-.
[22] R. A. Alvarez-Puebla, E. Arceo, P. J. G. Goulet, J. J. Garrido, R. F. Aroca, *J. Phys. Chem. B* **2005**, *109*, 3787–3792.
[23] J. Jiang, K. Bosnick, M. Maillard, L. Brus, *J. Phys. Chem. B* **2003**, *107*, 9964–9972.
[24] H. Xu, E. J. Bjerneld, J. Aizpurua, P. Apell, L. Gunnarsson, S. Petronis, B. Kasemo, C. Larsson, F. Hook, M. Kall, *Proc. SPIE Int. Soc. Opt. Eng.* **2001**, *4248*, 35.
[25] L. Gunnarsson, E. J. Bjerneld, H. Xu, S. Petronis, B. Kasemo, M. Kall, *Appl. Phys. Lett.* **2001**, *78*, 802–804.
[26] V. P. Safanov, V. M. Shalaev, V. A. Markel, Y. E. Danilova, N. N. Lepeshkin, W. Kim, S. G. Rautian, R. L. Armstrong, *Phys. Rev. Lett.* **1998**, *80*, 1102.
[27] K. Kneipp, H. Kneipp, P. Corio, S. D. M Brown, K. Shafer, J. Motz, L. T. Perelman, E. B. Hanlon, A. Marucci, G. Dresselhaus, M. S. Dresselhaus *Phys. Rev. Lett.* **2000**, *84*, 3470–3473.
[28] D. A. Weitz, M. Oliveria, *Phys. Rev. Lett.* **1984**, *52*, 1433.
[29] K. Kneipp, H. Kneipp, G. Deinum, I. Itzkan, R. R. Dasari, M. S. Feld, *Appl. Spectrosc.* **1998**, *52*, 175–178.
[30] B. Vlc¡kova, X. J. Gu, M. Moskovits, *J. Phys. Chem. B* **1997**, *101*, 1588–1593.
[31] Y.-S. Li, Y. Wang, J. Cheng, *Vib. Spectrosc.* **2001**, 27, 65–72.
[32] K. Faulds, R. E. Littleford, D. Graham, G. Dent, W. E. Smith, *Anal. Chem.* **2004**, *76*, 592–598.
[33] Y.-S. Li, J. Cheng, Y. Wang, *Spectrochim. Acta Part A* **2000**, *56*, 2067—2072.
[34] W. E. Doering, S. Nie, *J. Phys. Chem. B* **2002**, *106*, 311–317.

  

[35] B. Vlckova, X. J. Gu, D. P. Tsai, M. Moskovits, *J. Phys. Chem.* **1996**, *100*, 3169–3174.
[36] M. Moskovits, B. Vlckova, *J. Phys. Chem. B* **2005**, *109*, 14755–14758.
[37] D. Graham, W. E. Smith, A. M. T. Linacre, C. H. Munro, N. D. Watson, P. C. White, *Anal. Chem.* **1997**, *69*, 4703–4707.
[38] Y. Saito, J. J. Wang, D. A. Smith, D. N. Batchelder, *Langmuir* **2002**, *18*, 2959–2961.
[39] R. P. Van Duyne, J. C. Hulteen, D. A. Treichel, *J. Chem. Phys.* **1993**, *99*, 2101–2115.
[40] V. L. Schlegel, T. M. Cotton, *Anal. Chem.* **1991**, *63*, 241–247.
[41] M. A. De Jesus, K. S. Giesfeldt, J. M. Oran, N. A. Hatab, N. V. Lavrik, M. J. Sepaniak, *Appl. Spectrosc.* **2005**, *59*, 1501–1508.
[42] P. M. Tessier, O. D. Velev, A. T. Kalambur, J. F. Rabolt, A. M. Lenhoff, E. W. Kaler, *J. Am. Chem. Soc.* **2000**, *122*, 9554–9555.
[43] D. M. Kuncicky, S. D. Christesen, O. D. Velev, *Appl. Spectrosc.* **2005**, *59*, 401–409.
[44] L. Baia, M. Baia, J. Popp, S. Astilean *J. Phys. Chem. B* **2006**, *110*, 23 982–23 986.
[45] C. Ruan, G. Eres, W. Wang, Z. Zhang, B. Gu, *Langmuir* **2007**, *23*, 5757–5760.
[46] S. Nie, S. R. Emory, *Science* **1997**, *275*, 1102–1106.
[47] K. Kneipp, Y. Wang, H. Kneipp, L. T. Perelman, I. Itzkan, R. R. Dasari, M. S. Feld, *Phys. Rev. Lett.* **1997**, *78*, 1667.
[48] M. Suzuki, Y. Niidome, Y. Kuwahara, N. Terasaki, K. Inoue, S. Yamada, *J. Phys. Chem. B* **2004**, *108*, 11660–11665.
[49] B. Nikoobakht, M. A. El-Sayed, *J. Phys. Chem. A* **2003**, *107*, 3372–3378.
[50] X. Zou, S. Dong, *J. Phys. Chem. B* **2006**, *110*, 21545–21550.
[51] S. Chattopadhyay, H.-C. Lo, C.-H. Hsu, L.-C. Chen, K.-H Chen, *Chem. Mater.* **2005**, *17*, 553–559.
[52] A. M. Schwartzberg, C. D. Grant, A. Wolcott, C. E. Talley, T. R. Huser, R. Bogomolni, J. Z. Zhang, *J. Phys. Chem. B* **2004**, *108*, 19191–19197.
[53] H. K. Park, J. K. Yoon, K. Kim, *Langmuir* **2006**, *22*, 1626–1629.
[54] R. Gupta, W. A. Weimer, *Chem. Phys. Lett.* **2003**, *374*, 302–306.
[55] K. W. Kho, Z. X. Shen, H. C. Zeng, K. C. Soo, M. Olivo, *Anal. Chem.* **2005**, *77*, 7462–7471.
[56] S. R. Emory, S. Nie, *J. Phys. Chem. B* **1998**, *102*, 493–497.
[57] Z. M. Sui, X. Chen, L. Y. Wang, L. M. Xu, W. C. Zhuang, Y. C. Chai, C. J. Yang, *Physica E* **2006**, *33*, 308–314.
[58] S. E. J. Bell, N. M. S. Sirimuthu, *J. Phys. Chem. A* **2005**, *109*, 7405–7410.
[59] C. H. Munro, W. E. Smith, M. Garner, J. Clarkson, P. C. White, *Langmuir* **1995**, *11*, 3712–3720.
[60] R. Foucault, R. L. Brike, J. R. Lombardi, *Langmuir* **2003**, *19*, 8818–8827.
[61] J. P. Heritage, J. G. Bergman, A. Pinczuk, J. M. Worlock, *Chem. Phys. Lett.* **1979**, *67*, 229.
[62] C. Y. Chen, E. Burstein, S. Lundquist, *Solid State Commun.* **1979**, *32*, 63.
[63] P. C. Andersen, M. L. Jacobson, K. L. Rowlen, *J. Phys. Chem. B* **2004**, *108*, 2148–2153.
[64] A. M. Michaels, M. Nirmal, L. E. Brus, *J. Am. Chem. Soc.* **1999**, *121*, 9932–9939.
[65] K. Kalyanasundaram, J. K. Thomas, *J. Phys. Chem.* **1976**, *80*, 1462–1473.
[66] G. Wei, L. Wang, H. Zhou, Z. Liu, Y. Song, Z. Li, *Appl. Surf. Sci.* **2005**, *252*, 1189–1196.
[67] P. Hildebrandt, M. Stockberger, *J. Phys.Chem.* **1984**, *24*, 5935.
[68] M. Kahraman, M. M. Yazici, F. Sahin, Ö. F. Bayrak, M. Çulha, *Appl. Spectrosc.* **2007**, *61*, 479–485.
[69] M. Kahraman, M. M. Yazici, F. Sahin, M. Çulha, *J. Biomed. Opt.* **2007**, *12*, 054 015 (1–6).

Received: January 4, 2008
Published online on March 25, 2008

  